Dynamic structure factor for a two-component model plasma

A. Selchow,* G. Röpke, and A. Wierling
FB Physik, University of Rostock, Universitätsplatz 3, D-18051 Rostock, Germany†

H. Reinholz
Department of Physics, The University of Western Australia, Nedlands WA 6907, Australia

T. Pschiwul and G. Zwicknagel
Institut für Theoretische Physik, Universität Erlangen, Staudtstrasse 7, D-91058 Erlangen, Germany
(Received 15 June 2001; published 24 October 2001)

Analytical results for the structure factor of a two-component model plasma that describe an electron-ion plasma with modified interaction are derived from a Green function approach in different approximations. The random-phase approximation is improved by including the dynamic collision frequency, and results for the long-wavelength limit are extended to arbitrary wave numbers using the Mermin ansatz. After taking the classical limit of the resulting expressions, they are compared with molecular dynamics simulation results for the classical two-component model plasma.

DOI: 10.1103/PhysRevE.64.056410 PACS number(s): 52.25.Mq, 05.30.Fk, 71.45.Gm

I. INTRODUCTION

The two-component plasma (TCP) is an interesting system because it can model properties of different real plasmas, in particular hydrogen or the electron-hole plasma. It consists of two species c [e.g., electrons e and protons (ions) i] with masses m_c and charges e_c, and the interaction is given by the Coulomb potential $V_{cd}^C(r)=e_c e_d/(4\pi\epsilon_0 r)$. In equilibrium it is described by the temperature T and the densities n_c. For simplicity we assume singly charged ions, $e_i=-e_e=e$, and charge neutrality, $n_i=n_e=n$. The properties of such a system can be evaluated using the methods of quantum statistics [1]. Linear response properties have recently been considered by Reinholz *et al.* [2], denoted below as paper I. These many-particle approaches are based on a perturbative treatment of the Coulomb interaction. After performing partial summations, results are found which are exact in the limiting case of weak coupling, $\Gamma \ll 1$, and which can be used to find interpolations applicable in a large region of the parameters T,n. Here, the coupling parameter $\Gamma=e^2/(4\pi\epsilon_0 k_B T)(4\pi n/3)^{1/3}$ describes the ratio of potential energy and kinetic energy.

On the other hand, the properties of strongly correlated classical many-body systems can be successfully modeled by fully numerical treatments. As they are not restricted to parameter regions where approximations within perturbation theory are applicable, they can be used to verify analytical results, e.g., at strong coupling $\Gamma \geqslant 1$. For instance, the dynamic structure factor of a TCP-like system was evaluated by Pschiwul and Zwicknagel [3,4] using molecular dynamics (MD) computer simulations, where the classical equations of motion are solved numerically for an appropriate number of point particles. But in general, quantum effects have to be taken into account which arise (i) due to the symmetry properties for states of identical particles, and (ii) due to the uncertainty principle. As long as the density is lower than the degeneration density, effects of the symmetry (such as Pauli blocking) can be neglected, and the Fermi distribution function can be replaced by the Maxwell distribution. The uncertainty principle is of relevance in particular for interacting particles at short distances. Within a quasiclassical approximation, the Coulomb interaction can be replaced by an effective interaction which corresponds to a spatial average over distances characterized by the thermal wavelengths. Such quasiclassical effective interactions were derived by Kelbg [5] and by Deutsch [6] from quantum statistical expressions (Slater sums, see [1]).

In this paper we will consider the general form of the interaction

$$V_{cd}^{\Lambda}(r)=\frac{e_c e_d}{4\pi\epsilon_0 r}(1-e^{-r/\Lambda_{cd}}), \tag{1}$$

where Λ_{cd} are free parameters that define the model plasma. By taking $\Lambda_{cd}=(2\pi\hbar^2/m_{cd}k_B T)^{1/2}$, with $m_{cd}^{-1}=m_c^{-1}+m_d^{-1}$, we retrieve the quasiclassical effective interaction of [5,6] as discussed above. This modified potential avoids the Coulomb collapse in a classical treatment of the system. But it is still an unsolved problem whether and under which conditions a quasiclassical MD simulation based on interaction (1) can reproduce the dynamic properties of a TCP that has to be treated by quantum statistics. We will not discuss this open question either. Instead, we consider in the following a system where the Λ_{cd} are given fixed parameters. This model system of charged particles interacting via the potential (1) will be denoted as a two-component model plasma (TCMP). In particular we are interested in the well defined classical limit of this system, formally obtained if the limit $\hbar \to 0$ is considered. This classical two-component model plasma (CTCMP) can be rigorously treated by classical mechanics and MD simulations. The available computational power allows, however, only rather small sampling times

*Email address: selchow@darss.mpg.uni-rostock.de
†FAX: +49 (0)381-498 2857.

and system sizes. In certain limiting cases such as high frequencies or low densities, simulations should be checked against analytical results which then may represent better approximations. In the present work, MD simulations of the dynamic structure factor for a CTCMP will be compared with analytical results, and the validity of different approaches will be discussed.

Therefore, in Secs. II–IV we first derive analytical expressions for the TCMP by extending the quantum statistical treatment of a system interacting via the Coulomb potential (TCP), as given in (I), to systems with the effective interaction (1). In their classical limit these expressions then describe the CTCMP and allow an adequate comparison with MD simulations. This will be done in Sec. VI, after a discussion of the CTCMP and the MD simulation technique in Sec. V. The final conclusions are drawn in Sec. VII.

II. DYNAMIC RESPONSE OF A TWO-COMPONENT MODEL PLASMA

We consider a nonrelativistic charged particle system with components c (mass m_c, charge e_c, spin s_c) described by the Hamiltonian

$$H=\sum_{p,c} E_p^c a_{p,c}^\dagger a_{p,c} + \frac{1}{2}\sum_{pp'q,cc'} V_{cc'}(q) a_{p-q,c}^\dagger a_{p'+q,c'}^\dagger a_{p',c'} a_{p,c}. \quad (2)$$

$E_p^c=\hbar^2p^2/(2m_c)$ is the kinetic energy, $V_{cc'}(q)$ is an (arbitrary) interaction potential, and $a_{p,c}^\dagger$ denotes the creation operator of a particle of component c with momentum $\hbar\vec{p}$. In particular, we will restrict ourselves to a two-component (hydrogenlike) plasma consisting of electrons and ions (protons) so that $c=e,i$. The spin variable is included in the index c, and spin summations are performed in the final expressions.

In the case of the TCMP, the interaction is obtained from Eq. (1) as the Fourier transform

$$V_{cc'}(q)=V_{cc'}^\Lambda(q)=\frac{e_c e_{c'}}{\epsilon_0\Omega_0(q^2+\Lambda_{cc'}^2 q^4)}, \quad (3)$$

where Ω_0 is the normalization volume. The Coulomb interaction (TCP) is included as a special case when $\Lambda_{cc'}=0$.

Important quantities are the partial equilibrium correlation functions of the Fourier transform of local density fluctuations $\delta n_k^c=\Omega_0^{-1}\Sigma_p \delta n_{p,k}^c$ with the fluctuations of occupation numbers $\delta n_{p,k}^c=a_{p-k/2,c}^\dagger a_{p+k/2,c}-\langle a_{p-k/2,c}^\dagger a_{p+k/2,c}\rangle_{\rm eq}$,

$$\chi_{cc'}(\vec{k},\omega)=\Omega_0\frac{i}{\hbar}\int_0^\infty dt e^{i(\omega+i\eta)t}\langle[\delta n_k^c(t),\delta n_k^{c'}]\rangle_{\rm eq}. \quad (4)$$

Further equivalent definitions in terms of correlation functions can be found, e.g., in Ref. [1].

Related quantities are the density-density response function $\chi_{nn}(\vec{k},\omega)=\Sigma_{cc'}\chi_{cc'}(\vec{k},\omega)$ and the charge-charge density response function $\chi_{qq}(\vec{k},\omega)=\Sigma_{cc'}e_c e_{c'}\chi_{cc'}(\vec{k},\omega)$. The relation to the charge-density dynamic structure factor is

$$S_{qq}(\vec{k},\omega)=\frac{\hbar}{n}\frac{1}{1-e^{-\beta\hbar\omega}}\,{\rm Im}\,\chi_{qq}(\vec{k},\omega). \quad (5)$$

In the long-wavelength limit ($k\to 0$), a collision frequency $\nu(\omega)$ can be introduced in connection with a generalized Drude formula for the dynamic conductivity, for details see paper I. With the plasma frequency $\omega_{\rm pl}^2=\Sigma_c e_c^2 n_c/(\epsilon_0 m_c)$ we have

$$\nu(\omega)=-i\epsilon_0 k^2\frac{\omega_{\rm pl}^2}{\omega}\frac{1}{\chi_{qq}(0,\omega)}-i\frac{\omega_{\rm pl}^2}{\omega}+i\omega. \quad (6)$$

The use of perturbation theory to calculate the partial response functions (4) and the related quantities will be discussed in Sec. III. We give here only the lowest orders of perturbation theory, where we find the well-known result for the polarization function [7]

$$\chi_{cc'}^0(\vec{k},\omega)=\delta_{cc'}\frac{1}{\Omega_0}\sum_p\frac{f_{p+k/2}^c-f_{p-k/2}^c}{\Delta E_{p,k}^c-\hbar(\omega+i\eta)}=\chi_c^0(\vec{k},\omega)\delta_{cc'}, \quad (7)$$

where $\Delta E_{p,k}^c=E_{p+k/2}^c-E_{p-k/2}^c=\hbar^2\vec{k}\cdot\vec{p}/m_c$, $f_p^c=[\exp(\beta E_p^c-\beta\mu_c)+1]^{-1}$ denotes the Fermi distribution function, $\beta=1/(k_BT)$ is the inverse temperature, and μ_c is the chemical potential of species c. The limit $\eta\to 0$ has to be taken after the thermodynamic limit. Analytical expressions for various limiting cases can be found in [8]. In particular, we have $\lim_{k\to 0}\chi_c^0(k,\omega)=n_c k^2/(m_c\omega^2)$ and $\lim_{k\to 0}\chi_c^0(\vec{k},0)=-\beta n_c$. The standard random-phase approximation (RPA) is introduced performing summation over ring diagrams [9], equivalent to the introduction of a screened interaction $V_{cc'}^{\rm sc}(\vec{k},\omega)=V_{cc'}(\vec{k})+\Sigma_d V_{cd}(\vec{k})\chi_d^0(\vec{k},\omega)\Omega_0 V_{dc'}^{\rm sc}(\vec{k},\omega)$. Solving

$$\chi_{cc'}^{\rm RPA}(\vec{k},\omega)=\chi_c^0(\vec{k},\omega)\delta_{cc'}+\chi_c^0(\vec{k},\omega)\Omega_0 V_{cc'}^{\rm sc}(\vec{k},\omega)\chi_{c'}^0(\vec{k},\omega)$$

we find the RPA expression, cf. [4]

$$\chi_{ee}^{\rm RPA}(\vec{k},\omega)=\frac{\chi_e^0-\chi_e^0\Omega_0 V_{ii}\chi_i^0}{1-\chi_e^0\Omega_0 V_{ee}-\chi_i^0\Omega_0 V_{ii}+\chi_e^0\chi_i^0\Omega_0^2(V_{ee}V_{ii}-V_{ei}^2)}, \quad (8)$$

$$\chi_{ei}^{\rm RPA}(\vec{k},\omega)=\frac{\chi_e^0\Omega_0 V_{ei}\chi_i^0}{1-\chi_e^0\Omega_0 V_{ee}-\chi_i^0\Omega_0 V_{ii}+\chi_e^0\chi_i^0\Omega_0^2(V_{ee}V_{ii}-V_{ei}^2)},$$

and the corresponding expressions interchange e and i. The dependence on $\vec{k},\omega$ has been dropped. The complete RPA expression for the TCMP with model interaction (1) follows as

$$\chi_{qq}^{\mathrm{RPA}}(\vec{k},\omega) = \frac{\chi_e^0+\chi_i^0-\chi_e^0\chi_i^0\Omega_0(V_{ii}+V_{ee}+2V_{ei})}{1-\chi_e^0\Omega_0 V_{ee}-\chi_i^0\Omega_0 V_{ii}+\chi_e^0\chi_i^0\Omega_0^2(V_{ee}V_{ii}-V_{ei}^2)}. \tag{9}$$

In the special case $\Lambda_{cc'}=0$ (i.e., the case of the TCP with Coulomb interaction), the expressions simplify considerably since the interactions between the different species have the same q behavior, depending on the species via the charges e_c only.

III. PERTURBATION EXPANSION FOR THE INVERSE RESPONSE FUNCTION AND DYNAMIC COLLISION FREQUENCY

The inverse response function $M(\vec{k},\omega)$, defined by

$$\chi_{qq}(\vec{k},\omega)=i\beta\Omega_0\frac{k^2}{\omega}\frac{1}{M(\vec{k},\omega)}, \tag{10}$$

can be expressed in terms of correlation functions allowing for a systematic evaluation within perturbation theory, see paper I and further references given there. In the first order with respect to the interaction, the RPA expressions are obtained. Collisions within the system are described considering the second and higher orders of perturbation theory.

The evaluation of the second order of $M(\vec{k},\omega)$ for arbitrary $\vec{k},\omega$ is rather complex. As a special case, we consider the long-wavelength limit $k\to 0$, as done in paper I, where simple analytical expressions can be given. With $\chi_c^0(0,\omega)$ given above and $\lim_{k\to 0} V_{cc'}(k)\propto k^{-2}$ for the long-range potentials considered here, we have according to paper I for the dynamic collision frequency (6)

$$\nu(\omega)=\frac{\beta\Omega_0}{\epsilon_0\omega_{\mathrm{pl}}^2}\sum_{cc'}\frac{e_c e_{c'}}{m_c m_{c'}}F_{cc'}(\omega), \tag{11}$$

with the dynamic force-force correlation function

$$F_{cc'}(\omega)=\frac{1}{\Omega_0^2}\sum_{pp'qq'p_1p_1'dd'}V_{cd}(q)V_{c'd'}(q')q_z q_z' \times\langle a^\dagger_{p-q/2,c}a^\dagger_{p_1+q/2,d}a_{p_1-q/2,d}a_{p+q/2,c};a^\dagger_{p'+q'/2,c'}a^\dagger_{p_1'-q'/2,d'}a_{p_1'+q'/2,d'}a_{p'-q'/2,c'}\rangle_{\omega+i\eta}, \tag{12}$$

where $(q_z=\vec{q}\cdot\vec{k}/k)$. Using perturbation theory, results for the force-force correlation function will be given below in different approximations. For a TCP with Coulomb interaction, the static limit $\omega\to 0$ yielding the dc conductivity was considered in different works, see [10], in particular [11] for the electron-ion plasma. The extension to finite frequencies for the Coulomb interaction considered in paper I will be generalized here for arbitrary long-range interactions $V_{cc'}(q)$.

A. Born approximation

The evaluation of the force-force correlation function (12) in the Born approximation, see paper I for details, gives for $c'=c$

$$F_{cc}^{\mathrm{Born}}(\omega)=\frac{i\hbar}{\beta\Omega_0^2}\sum_{pqp'd}\frac{e^{\beta(\Delta E^d_{p',q}-\Delta E^c_{p,q})}-1}{\Delta E^d_{p',q}-\Delta E^c_{p,q}}q_z^2V_{cd}^2(q) \times\frac{f^d_{p'+q/2}(1-f^d_{p'-q/2})f^c_{p-q/2}(1-f^c_{p+q/2})}{\hbar(\omega+i\eta)+\Delta E^d_{p',q}-\Delta E^c_{p,q}} \times[1-\delta_{cd}]. \tag{13}$$

Exchange terms are neglected. Only a contribution for $d\neq c$ remains. For $c'=d\neq c$ we find the same expression as above with the opposite sign, and we have $F_{ee}^{\mathrm{Born}}(\omega)=F_{ii}^{\mathrm{Born}}(\omega)=-F_{ei}^{\mathrm{Born}}(\omega)$. According to Eq. (11), the dynamic collision frequency in the Born approximation follows as

$$\nu^{\mathrm{Born}}(\omega)=\frac{4\beta\Omega_0}{nm_{ei}}F_{ee}^{\mathrm{Born}}(\omega), \tag{14}$$

replacing in Eq. (13) c by e and d by i. The factor 4 is due to the summation over spin variables, $s_e=s_i=1/2$. For the TCMP with interaction (1) the high-frequency behavior can be evaluated as

$$\lim_{\omega\to\infty}\mathrm{Re}\,\nu^{\Lambda,\mathrm{Born}}(\omega) \propto\frac{e^{-\beta\hbar\omega/2}-e^{\beta\hbar\omega/2}}{\hbar\omega}\int d^3q\frac{q^2}{3}V_{ei}^{\Lambda^2}(q)\int d^3p \times\delta\left(\hbar\omega-\frac{\hbar^2\vec{p}\cdot\vec{q}}{m_e}\right)\exp\left[-\beta\left(\frac{\hbar^2p^2}{2m_e}+\frac{\hbar^2q^2}{8m_e}\right)\right] \propto\frac{e^{-\beta\hbar\omega/2}-e^{\beta\hbar\omega/2}}{\hbar\omega}\frac{q^3}{(q^2+\Lambda_{ei}^2q^4)^2} \times\exp\left[-\beta\left(\frac{\omega^2m_e}{2q^2}+\frac{\hbar^2q^2}{8m_e}\right)\right]\Bigg|_{q=\sqrt{2m_e\omega/\hbar}}\propto\omega^{-7/2}, \tag{15}$$

where a saddle-point approximation has been applied. It differs from the TCP case with Coulomb interaction where $\mathrm{Re}\,\nu^{\mathrm{TCP,Born}}(\omega)\propto\omega^{-3/2}$ was derived (paper I), which is related to the different behavior of the interaction potentials at large values of q.

The Born approximation for the dynamic collision frequency has to be improved (i) considering dynamic screening, which is of importance at small values of q and gives a reduction of the dynamic collision frequency especially at low frequencies, (ii) considering strong collisions being important at large values of q, (iii) considering renormalization, which is of importance particularly below the plasma frequency.

B. Dynamic screening

The interaction in the TCP as well as in the TCMP is long ranged so that the Fourier transform behaves as $\lim_{q\to 0} V(q)\propto q^{-2}$. Screening is then essential to avoid the singularity of the collision integral at $q\to 0$, which leads to a divergent static collision frequency $\nu^{\mathrm{Born}}(0)$. According to Fig. 2 of paper I, we have to sum up ring diagrams in evaluating the Green function describing the force-force correlation function. Using the spectral representation for the density-density correlation function we find $(n_B(\omega)=[\exp(\beta\hbar\omega)-1]^{-1})$

$$\nu^{\mathrm{RPA}}(\omega)=i\frac{\hbar}{\Omega_0 n m_{ei}}\sum_q\frac{q^2}{3}V_{ei}(q)V_{ei}(q)\int\frac{d\omega'}{\pi}\int\frac{d\omega''}{\pi}\times\frac{n_B(\omega')-n_B(-\omega'')}{(\omega+i\eta+\omega'+\omega'')(-\omega'-\omega'')}\times[\mathrm{Im}\,\chi_{ee}(q,\omega'+i\eta)\mathrm{Im}\,\chi_{ii}(-q,\omega''+i\eta)-\mathrm{Im}\,\chi_{ei}(q,\omega'+i\eta)\mathrm{Im}\,\chi_{ie}(-q,\omega''+i\eta)],\tag{16}$$

where the RPA expression (8),

$$\mathrm{Im}\,\chi_{ee}^{\mathrm{RPA}}(\vec{k},\omega)=\frac{\mathrm{Im}\,\chi_e^0[1-2V_{ii}\,\mathrm{Re}\,\chi_i^0+V_{ii}^2|\chi_i^0|^2]+\mathrm{Im}\,\chi_i^0V_{ei}^2|\chi_e^0|^2}{|1-\chi_e^0V_{ee}-\chi_i^0V_{ii}+\chi_e^0\chi_i^0(V_{ee}V_{ii}-V_{ei}^2)|^2},$$

$$\mathrm{Im}\,\chi_{ei}^{\mathrm{RPA}}(\vec{k},\omega)=\frac{\mathrm{Im}\,\chi_e^0[V_{ei}\,\mathrm{Re}\,\chi_i^0-V_{\mathrm{ei}}V_{ii}|\chi_i^0|^2]+\mathrm{Im}\,\chi_i^0[V_{ei}\,\mathrm{Re}\,\chi_e^0-V_{ei}V_{ee}|\chi_e^0|^2]}{|1-\chi_e^0V_{ee}-\chi_i^0V_{ii}+\chi_e^0\chi_i^0(V_{ee}V_{ii}-V_{\mathrm{ei}}^2)|^2},\tag{17}$$

and corresponding expressions interchanging e and i can be used to describe the dynamic screening of the interaction.

For a TCP with a Coulomb interaction the expressions (17) are simplified. In that case, the Lenard-Balescu collision integral follows in the zero-frequency limit. The RPA result can be improved determining $\chi_{cc'}(q,\omega)$ in Eq. (16) in a self-consistent way, using the result derived below which takes the effect of collisions into account, see Sec. IV. The Born result is recovered replacing $\chi_{cc'}(q,\omega)$ in Eq. (16) by $\chi_{cc'}^0(q,\omega)$.

The divergence of $\nu^{\mathrm{Born}}(0)$ for long-range interactions is already avoided if instead dynamic screening a statically screened potential is used, replacing $V_{cc'}(q)$ by $V_{cc'}(q)/(1+\kappa^2/q^2)$ with the screening parameter $\kappa^2=ne^2/(\epsilon_0k_BT)$. Introducing dimensionless quantities, we have (see Ref. [2])

$$\nu^{\Lambda,\mathrm{Born}}(\omega)=-ign\int_0^\infty dy\,\frac{y^4}{(y^2+\overline{n})^2(1+\overline{\Lambda}_{ei}^2y^2)^2}\times\int_{-\infty}^{\infty}dx\,\frac{\exp[-(x-y)^2](1-\exp[-4xy])}{xy(xy-w-i\eta)},\tag{18}$$

$$g=\frac{1}{24\sqrt{2}\pi^{5/2}}\frac{e^4\beta^{3/2}}{m_e^{1/2}\epsilon_0^2},\quad w=\frac{\hbar\omega}{4k_BT},\quad \overline{n}=\frac{\hbar^2\kappa^2}{8m_ek_BT},$$

where in comparison with Eq. (48) in paper I the normalized potential parameter $\overline{\Lambda}_{ei}=\sqrt{8m_e/\hbar^2\beta}\Lambda_{ei}$ appears. In the zero-frequency limit $\omega=0$ a Ziman-Faber-like expression is obtained, Eq. (18),

$$\nu^{\Lambda,\mathrm{ZF}}=\nu^{\Lambda,\mathrm{Born}}(0)=4\pi gn\int_0^\infty dy\,\frac{y^3e^{-y^2}}{(1+\overline{\Lambda}_{ei}^2y^2)^2(y^2+\overline{n})^2}.\tag{19}$$

Results for the dynamic collision frequency in different approximations are shown in Fig. 1, lower part, for the parameter value $\Gamma=2.0$. The data are normalized with the plasma frequency $\omega_{\mathrm{pl},e}=(ne^2/\epsilon_0m_e)^{1/2}$. While the static expression $\nu^{\Lambda,ZF}$ is a real constant, the dynamic expression $\nu^{\Lambda,\mathrm{Born}}(\omega)$ and $\nu^{\Lambda,\mathrm{RPA}}(\omega)$ are complex, frequency-dependent functions. The dynamic screening of the collisions in $\nu^{\Lambda,\mathrm{RPA}}(\omega)$ leads to strong deviations from the static screening $\nu^{\Lambda,\mathrm{Born}}(\omega)$ near the plasma frequency.

C. Strong collisions

Up to now the dynamic collision frequency was given in the Born approximation with respect to a static long-range interaction $V_{cc'}(q)$ or the dynamically screened interaction. However, the Born approximation is limited to weak scattering. To treat strong collisions, a ladder-T matrix approximation has to be considered, see paper I, describing binary col-

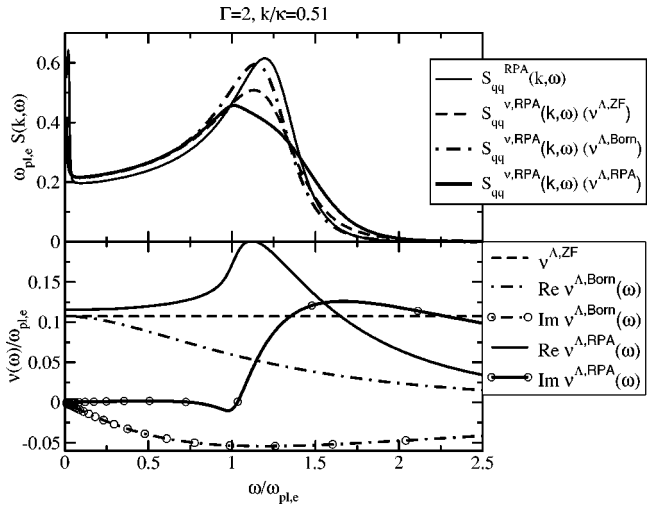

FIG. 1. The influence of the dynamic collision frequency $\nu(\omega)$ (lower part) on the dynamic structure factor $S_{qq}(k,\omega)/e^2$, for the CTCMP (upper part) [Eqs. (9) and (25)]. Different approximations for $\nu(\omega)$ are considered: the static Ziman-Faber [Eq. (19)] (dashed line), the statically screened [Eq. (18)] (dot-dashed line), and the dynamically screened [Eq. (16)] result (full line). The parameter values are $\Gamma=2$, $k/\kappa=0.51$.

lisions. For a two-component plasma within an adiabatic approximation, the contribution to the collision frequency due to a partial summation of ladder diagrams reads

$$\nu^T(\omega)=\frac{i\hbar}{\Omega_0 n m_{ei}}\sum_{nn'P}\times\frac{e^{\beta(E_{nP}-E_{n'P})}-1}{E_{nP}-E_{n'P}}\frac{g(E_{nP})[1+g(E_{n'P})]}{\hbar(\omega+i\eta)+E_{nP}-E_{n'P}}\times\left|\sum_{p_e,p_i,q}\psi^*_{n'P}(p_e,p_i)V(q)q_z\psi_{nP}(p_e+q,p_i-q)\right|^2. \tag{20}$$

Here, $g(E)$ is the two-particle distribution function and ψ_{nP} are solutions of the Schrödinger equation for an appropriate potential $V(q)$ to be specified below. Equation (20) shows that the collision frequency is given in terms of dipole matrix elements.

A classical limit of this expression can be obtained using the WKB approximation for the wave functions. As shown in [12], the WKB approximation for the Coulomb wave function reproduces the classical trajectory in a Coulomb potential.

In the dynamically screened binary collision approximation for the collision frequency $\nu(\omega)$, the ladder-T matrix should be calculated for the dynamically screened interaction instead of the static one, what can be done in a certain approximation summing up the different expressions (16) and (20), see paper I. To avoid interferences with dynamic screening and double counting, Gould and DeWitt [14] proposed to add the difference of the T-matrix result and the Born result to the dynamically screened Born approximation. Within this approach, the wave functions are determined using a statically screened Coulomb potential in the case of a TCP. For the TCMP, the modified potential given by Eq. (1) is weak compared to the Coulomb potential. Thus, it is expected that the difference between the T-matrix approximation and the Born approximation is small.

In the high-frequency limit, the Born approximation converges to the T-matrix approximation. Hence, we estimate the difference by comparing with the static value of the collision frequency given by

$$\nu^T(0)=\frac{8}{3\sqrt{2\pi}}\frac{n_i\beta^{5/2}}{m_e^{1/2}}\int_0^\infty dE E^2 e^{-\beta E}Q(E). \tag{21}$$

Here, $Q(E)$ denotes the transport cross section for a given collision energy E. Within a partial wave expansion it is determined from the phase shifts via

$$Q(E)=\frac{4\pi\hbar^2}{m_e E}\sum_{l=0}^{\infty}(l+1)\sin^2[\delta_l(k)-\delta_{l+1}(k)]. \tag{22}$$

We have compared the collision frequency using phase shifts in the Born and in the WKB approximation, see [13], with respect to a static screened model potential for the collision between ions and electrons $V_{ei}^{D,\Lambda}(q)=q^2(q^2+\kappa^2)^{-1}V_{ei}^{\Lambda}(q)$. Here, κ^{-1} denotes the Debye screening length. For the conditions given in Sec. VI the differences are small amounting to 25% at largest. Thus, within the errors of the simulation data, the use of the dynamically screened Born approximation is sufficient.

D. Renormalization factor

Evaluating the dynamic collision frequency $\nu(\omega)$, the dynamically screened binary collision approximation which is based on the evaluation of the force-force correlation function (12) will not give the correct result in the low-density limit when the plasma is nondegenerate. To obtain the correct limit, all moments of the ion and electron distribution functions have to be taken into account to describe the nonequilibrium state.

Up to now we have considered only the particle current densities as relevant observables. Higher moments of the electron and ion distribution function also will contribute to the evaluation of the dynamic structure factor. They can be incorporated by a renormalization factor $r(\omega)$, which was introduced in [15]. Expressions for $r(\omega)$, which is a complex function, can be found in paper I. According to Fig. 11 of paper I, the effect of the renormalization factor, modifying the collision frequency calculated in the dynamically screened binary collision approximation, is up to 20% near k_BT and the factor approaches 1 in the limit of large frequencies, leaving the asymptotic behavior $\lim_{\omega\to\infty}\mathrm{Re}\,\nu(\omega)\propto\omega^{-7/2}$ unchanged.

IV. RESPONSE FUNCTION AT FINITE WAVE NUMBERS AND THE MERMIN ANSATZ

The evaluation of the response function or the corresponding dynamic collision frequency was given in Sec. III

only in the long-wavelength limit. Microscopic expressions can also be given for finite wave numbers $\vec{k}$, see paper I; its evaluation, however, is very tedious. We will apply a semiphenomenological approach to evaluate the response function at finite wave numbers.

According to Mermin [16], collisions can be taken into account in the polarization function in a phenomenological way as follows: (i) Start with the RPA expression (8) for the collisionless plasma. (ii) Replace the frequency ω by the complex variable $\omega+i/\tau$ where the real number τ has the meaning of a relaxation time which can be introduced in a phenomenological way. (iii) To fulfill conservation laws, in particular the conservation of particle numbers, an expression for the polarization function can be considered,

$$\chi_c^{\mathrm{M},0}(k,\omega)=(1-i\omega\tau)\left(\frac{\chi_c^0(k,\omega+i/\tau)\chi_c^0(k,0)}{\chi_c^0(k,\omega+i/\tau)-i\omega\tau\chi_c^0(k,0)}\right). \tag{23}$$

A derivation of this result using the method of the nonequilibrium statistical operator [17] was given recently [18]. This way, a closer connection to the microscopic description can be given, and further conserved or slowly varying quantities can be taken into account, see also [19].

The inclusion of particle number conservation within the method of the nonequilibrium statistical operator allows also for a frequency-dependent relaxation time. This way, a result similar to Eq. (23) can be derived, where the inverse relaxation time $1/\tau$ is replaced by the complex collision frequency $\nu(\omega)$. Thus, in the long-wavelength limit the correct, microscopically calculated polarization function (paper I) will be reproduced. Therefore we expect that also for finite values of k a reasonable approximation is achieved.

The resulting Mermin polarization function, as derived in [18], is

$$\chi_c^{\nu,0}(k,\omega)=\left(1-\frac{i\omega}{\nu(\omega)}\right)\left(\frac{\chi_c^0(k,z)\chi_c^0(k,0)}{\chi_c^0(k,z)-\dfrac{i\omega}{\nu(\omega)}\chi_c^0(k,0)}\right), \tag{24}$$

$$z=\omega+i\nu(\omega)=\omega-\mathrm{Im}\,\nu(\omega)+i\,\mathrm{Re}\,\nu(\omega).$$

To get the RPA-Mermin susceptibility for a two-component system interacting via the potential $V_{cc}(q)$, we have to replace the polarization function $\chi_c^0(k,\omega)$ in Eq. (9) by Eq. (24). As a result we obtain

$$\chi_{qq}^{\nu,\mathrm{RPA}}(\vec{k},\omega)=\frac{\chi_e^{\nu,0}+\chi_i^{\nu,0}-\chi_e^{\nu,0}\chi_i^{\nu,0}\Omega_0(V_{ii}+V_{ee}+2V_{ei})}{1-\chi_e^{\nu,0}\Omega_0V_{ee}-\chi_i^{\nu,0}\Omega_0V_{ii}+\chi_e^{\nu,0}\chi_i^{\nu,0}\Omega_0^2(V_{ee}V_{ii}-V_{ei}^2)}. \tag{25}$$

(For shortness, ω and k have been dropped on the right-hand side.) It should be mentioned that for $k\to 0$ the correct microscopic expression for $\chi_{qq}(0,\omega)$, based on the given approximation for $\nu(\omega)$, is reproduced. Results for the response function $\chi_{qq}^{\nu,\mathrm{RPA}}(k,\omega)$ and the corresponding dynamic structure factor are given in Sec. VI.

V. THE CTCMP AND ITS NUMERICAL TREATMENT

Taking the limit $\hbar\to 0$ of the TCMP and all the previously derived expressions, we arrive at a well defined entirely classical description, the classical two-component model plasma (CTCMP), which is determined by the classical counterpart of the Hamiltonian (2)

$$\mathcal{H}=\sum_\alpha\frac{p_\alpha^2}{2m_\alpha}+\frac{1}{2}\sum_{\alpha,\beta\neq\alpha}\frac{e_\alpha e_\beta}{4\pi\epsilon_0|\vec{r}_\alpha-\vec{r}_\beta|}\times(1-\exp[-|\vec{r}_\alpha-\vec{r}_\beta|/\Lambda_{\alpha\beta}]). \tag{26}$$

Introducing now the scaling $\tilde{\mathcal{H}}=\mathcal{H}/k_BT$, $\tilde{p}=p/(m_ek_BT)^{1/2}$, and $\tilde{r}=r/a$ with $a=(4\pi n/3)^{-1/3}$, and the dimensionless parameters $\tilde{\Lambda}_{\alpha\beta}=\Lambda_{\alpha\beta}/a$, the Hamilton function (26) reads

$$\tilde{\mathcal{H}}=\sum_\alpha\frac{m_e}{m_\alpha}\frac{\tilde{p}_\alpha^2}{2}+\frac{\Gamma}{2}\sum_{\alpha,\beta\neq\alpha}\frac{e_\alpha e_\beta}{e^2|\tilde{\vec{r}}_\alpha-\tilde{\vec{r}}_\beta|}\times(1-\exp[-|\tilde{\vec{r}}_\alpha-\tilde{\vec{r}}_\beta|\tilde{\Lambda}_{\alpha\beta}]). \tag{27}$$

For fixed masses $m_i=m_p$ and m_e, and charges $e_i=-e_e=e$, the system depends on the parameters $\tilde{\Lambda}_{\alpha\beta}$, but on n,T only through the classical plasma parameter Γ. For $\tilde{\Lambda}_{\alpha\beta}\lesssim 1$, weakly coupled systems are characterized by $\Gamma\ll 1$ and nonideal ones by $\Gamma\gtrsim 1$. As the CTCMP can be completely treated by classical mechanics, molecular dynamics (MD) simulations, see, e.g., [20], provide a suitable tool to study the full many-body dynamics of these systems, in particular at $\Gamma\gtrsim 1$. During the last decades MD simulations have been successfully applied to various strongly coupled plasmalike systems as the classical one-component plasma (OCP) or (binary) ionic mixtures, see, e.g., [21–23]. The procedure is conceptually very simple: the N_i ions (protons) and N_e electrons $\{\vec{r}_\alpha,\ \vec{p}_\alpha,\ \alpha=1,...,N,\ N=N_i+N_e\}$ just follow the classical equations of motion with the mutual interactions (1)

$$\frac{d\tilde{\vec{r}}}{d\tilde{t}}=\frac{m_e}{m_\alpha}\tilde{\vec{p}}_\alpha,$$

$$\frac{d\tilde{\vec{p}}_\alpha}{d\tilde{t}}=-\frac{\partial}{\partial\tilde{\vec{r}}_\alpha}\left[\Gamma\sum_{\beta\neq\alpha}\frac{e_\alpha e_\beta}{e^2|\tilde{\vec{r}}_\alpha-\tilde{\vec{r}}_\beta|}\times(1-\exp[-|\tilde{\vec{r}}_\alpha-\tilde{\vec{r}}_\beta|/\tilde{\Lambda}_{\alpha\beta}])\right], \tag{28}$$

which are integrated numerically. The dynamics of the CTCMP, as given by the scaled dimensionless equations (28), with $\tilde{t}=t(k_BT/m_ea^2)^{1/2}$, depends only on the parameters Γ and $\tilde{\Lambda}_{\alpha\beta}$.

The MD simulations contain, without restrictions on the strength of the interaction, all correlation effects, dynamic

screening, close collisions, and multiparticle correlations. They do not rely on a spatial grid and there is no restriction in the spatial resolution. On the other hand, the expense grows quadratically with the particle number N because the long-ranged Coulomb part of the force is to be evaluated separately for each pair of particles. The available computing power thus limits the computation to at most a few thousand particles. In order to approximate an infinite system by a finite particle number, the particles are packed into an elementary cubic simulation box of length L and this box is continued periodically in all three spatial directions. Thus, a particle is replaced by a cubic lattice of particles and the Coulomb part of the interaction by an Ewald sum of Coulomb interactions [24,25]. The limited simulation box introduces, however, a largest length scale on which collective phenomena can be explored and a discrete set of allowed wave vectors $\vec{k}=2\pi\vec{n}/L$ with the smallest possible wave number $k=2\pi/L$. In units of the inverse screening length κ, i.e., the inverse of the Debye length $\kappa=1/\lambda_D=(ne^2/\epsilon_0 k_B T)^{1/2}$, $k/\kappa=2\pi\lambda_D/L$ scales like $k/\kappa \propto N^{-1/3}\Gamma^{-1/2}$. Thus small k/κ are only accessible for large Γ (and N). This limitation becomes a serious problem with decreasing Γ. But then one leaves the nonideal regime anyway and can continue with simpler methods. It is a general feature, that MD simulations are particularly suited for the case of strong coupling and become inefficient, if not impossible, just where weak coupling approaches are valid.

Equations (28) are solved using a standard velocity-Verlet algorithm [20]. But for particles which come very close to each other, in particular for the attractive ion-electron interaction, the arising large forces require a strong reduction of the time step which slows down the numerical propagation. This is avoided by introducing a separate treatment of close collisions, which takes advantage of the fact that the time scales in the close collision region are much shorter than those for the system as a whole. The close colliding particles are thus propagated as subsystems with a much reduced time step [26,27]. The accuracy and stability of the simulation runs are monitored using the total energy $\mathcal{H}$. The outlined scheme ensures the conservation of $\mathcal{H}$ with an accuracy typically better than 10^{-5} at a global time step $\Delta t=0.0086\omega_{\mathrm{pl},e}^{-1}$, where $\omega_{\mathrm{pl},e}=(ne^2/m_e\epsilon_0)^{1/2}=(3\Gamma)^{1/2}(k_B T/m_e a^2)^{1/2}$ is the electronic plasma frequency.

In MD simulations, observables are measured as time averages over a certain time interval and/or as ensemble averages over different initial configurations. To determine the dynamic structure factor from the classical trajectories $\{\vec{r}_\alpha(t)\}$ we first sample for different possible vectors $\vec{k}$ the Fourier transform $\rho_{\vec{k}}(t)=\Sigma_\alpha e_\alpha \exp[-i\vec{k}\cdot\vec{r}_\alpha(t)]$ of the charge density $\rho(\vec{r},t)=\Sigma_\alpha e_\alpha \delta^3[\vec{r}-\vec{r}_\alpha(t)]$ as a function of time. Then the density-density autocorrelation function $\Phi(\vec{k},t)$ is calculated from a time average over the simulation time τ and an ensemble average denoted by $\langle\,\rangle$ over different runs with varying initial microscopic configurations as

$$\Phi(\vec{k},t)=\frac{1}{N}\frac{1}{\tau}\int_0^\tau dt'\langle\rho_{\vec{k}}(t'+t)\rho_{-\vec{k}}(t')\rangle, \tag{29}$$

where $N=N_i+N_e$. Transforming $\Phi(\vec{k},t)$ into the frequency domain, we finally obtain the dynamic structure factor

$$\begin{aligned} S(\vec{k},\omega)&=\frac{1}{2n}\int d^3r\int_{-\infty}^{\infty}dt\langle\rho(\vec{r}'+\vec{r},t'+t)\\ &\quad\times\rho(\vec{r}',t')\rangle e^{-i(\vec{k}\cdot\vec{r}-\omega t)}\\ &=\int_{-\infty}^{\infty}dt\Phi(\vec{k},t)e^{i\omega t}, \end{aligned} \tag{30}$$

where $n=n_i=n_e$. Of course, this Fourier transform has to be performed numerically, which restricts the time integral in Eq. (30) to the simulation time τ and introduces the usual artifacts and problems related to numerical integral transformations [28]. We will resume this when comparing the MD results with the analytical treatment.

The actual simulations run with $N_i=N_e=250$ particles of each species with the proton-electron mass ratio $m_i/m_e=1836$ over a typical time of $\tau=360\omega_{\mathrm{pl}}^{-1}$. The dynamic structure factor is evaluated at constant total energy in an equilibrium state of the system, which is prepared by a preceding sufficiently long simulation at constant temperature. The shown results typically represent an ensemble average over 10,...,20 individual simulations. The error is deduced from the fluctuations in the ensemble of events. In all presented simulations the same parameters $\tilde{\Lambda}_{\alpha\beta}=\Lambda_{\alpha\beta}/a$ have been used. Guided by the quantum statistical derivation [5,6] of the effective potential (1) where $\Lambda_{\alpha\beta}\propto(m_{\alpha\beta})^{-1/2}$, we defined them through $\tilde{\Lambda}_{\alpha\beta}=(m_{ie}/m_{\alpha\beta})^{1/2}\tilde{\Lambda}_{ie}$ with a fixed $\tilde{\Lambda}_{ie}=0.4$ and the reduced masses $m_{\alpha\beta}=m_\alpha m_\beta/(m_\beta+m_\beta)$, i.e., $\tilde{\Lambda}_{ii}=0.013$ and $\tilde{\Lambda}_{ee}=0.57$.

VI. ANALYTICAL EXPRESSIONS VERSUS MD SIMULATION RESULTS

In the classical limit as investigated in the MD simulations the fluctuation-dissipation law (5) modifies to

$$S_{qq}(k,\omega)=-\frac{1}{n\beta\omega}\,\mathrm{Im}\,\chi_{qq}(k,\omega). \tag{31}$$

For the classical version of the response function $\chi_{qq}(k,\omega)$ we apply two different models, the common RPA (8) with $z=\omega$ and the RPA-Mermin susceptibility (25) with $z=\omega+i\nu(\omega)$ as frequency argument in $\chi_c^0(k,z)$ (7), which is taken in the limit $\hbar\to 0$ given by the expression

$$\chi_c^0(k,z)=-n_c\beta[1+i\sqrt{\pi}x_c w(x_c)], \tag{32}$$

with

$$x_c=\sqrt{\frac{m_c\beta}{2}}\,\frac{z}{k} \tag{33}$$

and

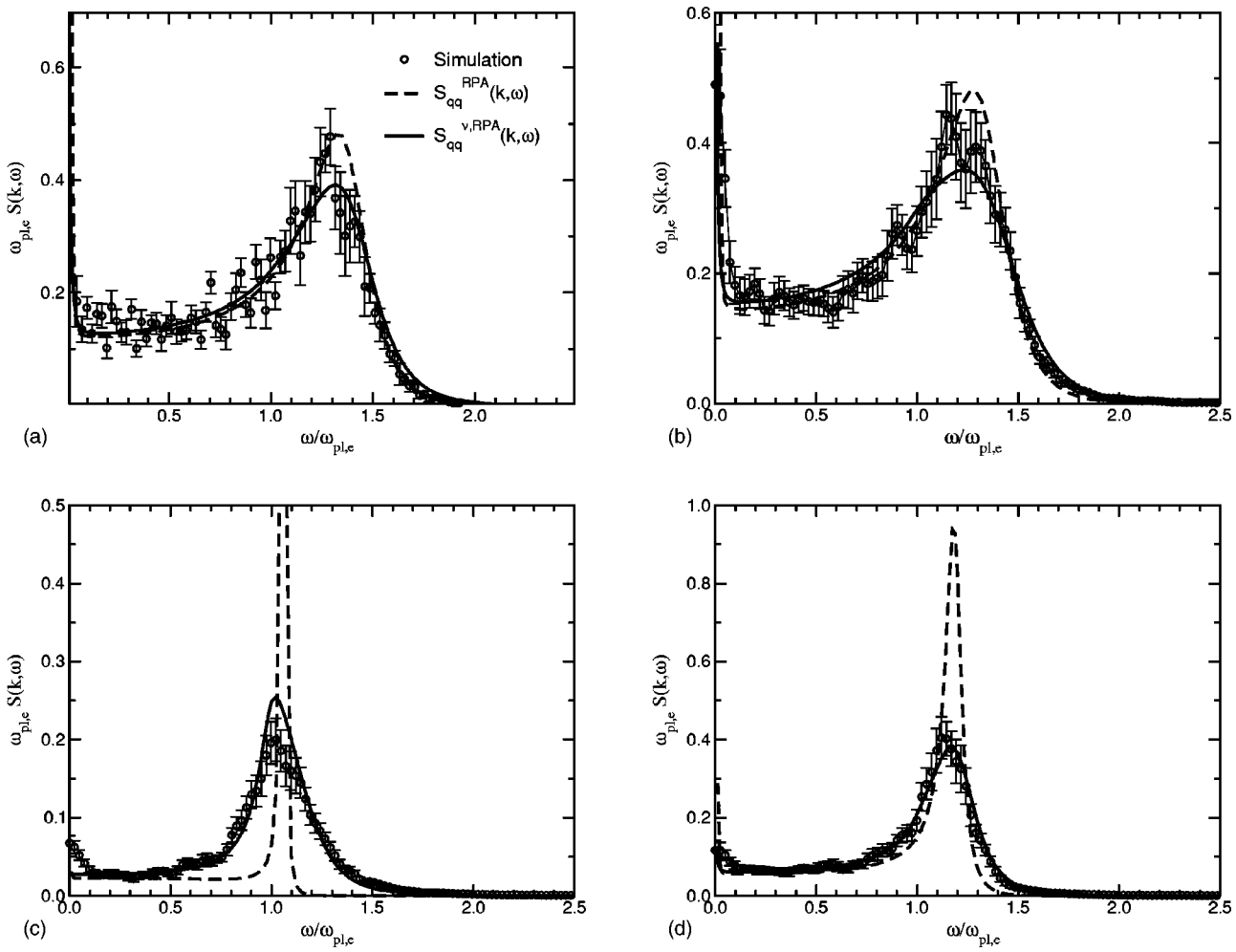

FIG. 2. Dynamic structure factor $S_{qq}(k,\omega)/e^2$ for an electron-proton model plasma in the RPA [Eq. (8)] and in the Mermin-like approximation [Eq. (25)] with dynamically screened dynamic collision frequency $\nu^{\Lambda,\mathrm{RPA}}(\omega)$, Eq. (16), for different parameter values of $\Gamma, k/\kappa$. (a) $\Gamma=0.5$, $k/\kappa=0.51$. (b) $\Gamma=1$, $k/\kappa=0.51$. (c) $\Gamma=2$, $k/\kappa=0.25$. (d) $\Gamma=1$, $k/\kappa=0.36$.

$$w(x)=\exp(-x^2)\left[1+\frac{2i}{\sqrt{\pi}}\int_0^x dt\,\exp(t^2)\right]. \qquad (34)$$

The influence on the dynamic collision frequency on the dynamic structure factor $S(k,\omega)$ is depicted in Fig. 1, upper part. We start from the collisionless RPA expression. Under the influence of the static $\nu^{\Lambda,\mathrm{ZF}}$ (19) the peak in the structure factor $S^{\nu,\mathrm{RPA}}(k,\omega)$ is broadened and slightly shifted towards lower frequencies. This effect is partially canceled by introducing the frequency-dependent static screening, leading to the dynamic $\nu^{\Lambda,\mathrm{Born}}(\omega)$ (18). The structure factor starts at the same static limit as the previous one but due to the vanishing values for $\nu^{\Lambda,\mathrm{Born}}(\omega)$ above $\omega_{\mathrm{pl},e}$ it merges with the RPA structure factor at higher frequencies. Hence, the peak has also a frequency shift but it appears smaller than in the case of a static $\nu^{\Lambda,\mathrm{ZF}}$. Improving the screening by dynamic contributions the peak becomes broader again and slightly asymmetric because the collision frequency $\nu^{\Lambda,\mathrm{RPA}}(\omega)$ (16) surpasses the static value $\nu^{\Lambda,\mathrm{ZF}}$ around $\omega_{\mathrm{pl},e}$ and decreases with the same asymptotic behavior as $\nu^{\Lambda,\mathrm{Born}}(\omega)$. Thus, the high frequency tail of $S^{\nu,\mathrm{RPA}}(k,\omega)$ with dynamically screened collision frequency lays above the other results.

In Fig. 2 the dynamic RPA-Mermin structure factor $S_{qq}^{\nu,\mathrm{RPA}}(k,\omega)$ (31), (25) with the dynamically screened collision frequency $\nu^{\Lambda,\mathrm{RPA}}(\omega)$ (16) is compared with the common RPA structure factor (8) and the results of the MD simulations (29),(30) at different Γ and k/κ values. The error bars to the MD data represent the fluctuations in the ensemble of individual simulation runs. With increasing Γ and decreasing k significant differences between the MD results and the collisionless RPA structure factor develop, indicating a much stronger damping of the plasmon mode at increasing nonideality of the TCMP. In contrast to the collisionless RPA the theoretical values for the dynamic RPA-Mermin structure factor follow this trend very well and are in very good agreement with the simulation data concerning position and width of the peak. Differences between the simulation data and $S_{qq}^{\nu,\mathrm{RPA}}(k,\omega)$ appear on the high frequency side for $k/\kappa=0.51$, where it seems that the influence of collisions are slightly overestimated at higher frequencies. In the case of smaller k values no such differences arise.

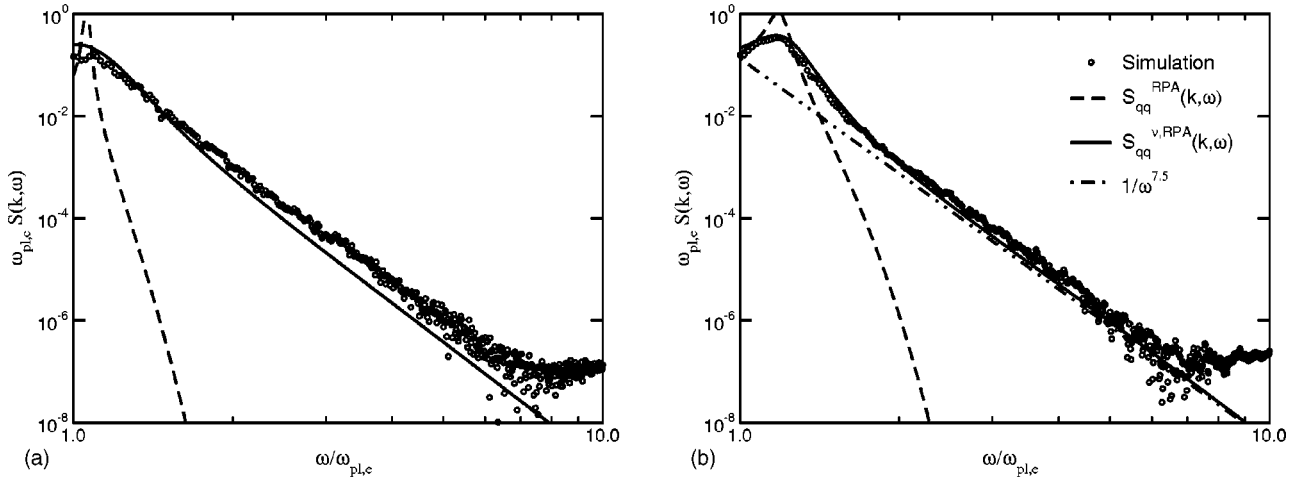

FIG. 3. Log-log plot of the dynamic structure factor $S_{qq}(k,\omega)/e^2$ and comparison with an asymptote $\sim 1/\omega^{7.5}$ [Eq. (15)] for different parameter values. (a) $\Gamma=2$, $k/\kappa=0.25$. (b) $\Gamma=1$, $k/\kappa=0.36$.

In Fig. 3 the asymptotic behavior of $S_{qq}(k,\omega)$ is investigated. While $S_{qq}^{\mathrm{RPA}}(k,\omega)$ vanishes exponentially the dynamic RPA-Mermin structure factor $S_{qq}^{\nu,\mathrm{RPA}}(k,\omega)$ drops down with the asymptote $1/\omega^{7.5}$ (15). This is again in good agreement with the simulation data. Due to the unavoidable fluctuations of the MD simulation data and the usual restrictions of numerical Fourier transforms, the accessible frequency domain for the dynamic structure factor as obtained from the simulations is, however, restricted to frequencies below ~ 5 to 10 $\omega_{\mathrm{pl},e}$.

But at even stronger coupling the present theoretical approach becomes questionable. For $\Gamma>2$ it starts to underestimate the influence of collisions as a damping mechanism, probably because only electron-ion collisions are included and pair correlation effects are neglected. Thus, for higher Γ values the theory predicts a more pronounced peak compared to the simulation, as shown for instance in Fig. 4.

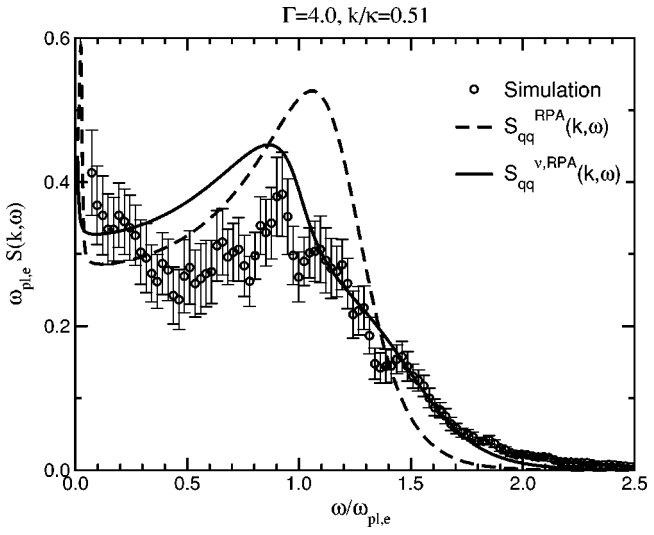

FIG. 4. Plot of the dynamic structure factor $S_{qq}(k,\omega)/e^2$ at strong coupling ($\Gamma=4, k/\kappa=0.51$). The Mermin-like approximation [Eq. (25)] overestimates the plasmon peak but is able to reproduce the high frequency tail of the simulation.

As an important test, we checked for the RPA-Mermin susceptibility (25) exact properties as, e.g., the sum rule

$$\frac{e^2}{\epsilon_0}\int_0^\infty d\omega\,\omega^2 S_{qq}(k,\omega) = -\frac{\pi}{2}\frac{k^2}{\kappa^2}\omega_{\mathrm{pl}}^2. \tag{35}$$

Table I shows the actual values as obtained for different parameters and demonstrates that the RPA-Mermin susceptibility obviously fulfills the *f*-sum rule within the numerical errors.

VII. CONCLUSIONS

Previous work concerning the response function in the long-wavelength limit and the dynamic collision frequency (paper) has been extended to finite wave numbers. For this the Mermin approach has been utilized which is based on the continuation of RPA expressions to complex frequencies ensuring conservation laws. In the present paper, microscopic approaches to the dynamic collision frequency were employed in order to incorporate the quantum statistical approach to the dynamic structure factor in the long-wavelength limit. The Mermin-like approach using a complex collision frequency appears to be a robust and feasible procedure, which guarantees exact properties such as

TABLE I. Check of the frequency sum rule [Eq. (35)] for $S_{qq}^{\nu,\mathrm{RPA}}(k,\omega)$ [Eq. (25)] with the dynamic collision frequency [Eq. (16)], corresponding to the parameter values considered in Figs. 2–4. The analytical integral value is normalized to 1.

Γ	k/κ	Sum
0.5	0.505	1.001
1.0	0.505	1.001
1.0	0.357	1.001
2.0	0.252	1.003
4.0	0.357	1.001

sum rules and reproduces the correct behavior in limiting cases.

The analytical approach has been compared with molecular-dynamics simulations. Because the MD simulations were done on the level of classical dynamics, a two-component model plasma was considered replacing the Coulomb potential by a model potential which allows for a classical limit. For this classical model plasma, MD simulations are an appropriate and powerful numerical tool for a treatment of the full many-body dynamics without restrictions on the strength of the interaction. They contain dynamic screening, close collisions, and multiparticle correlations and are particularly suited for investigating the dynamic properties of strongly coupled systems with $\Gamma \gtrsim 1$.

Comparing results for the dynamic structure factor we found that the analytical theory in the classical limit and the MD simulations are in good agreement for moderate values of the plasma parameter $\Gamma \lesssim 1$. Deviations arise for higher values of Γ as shown, e.g., for $\Gamma = 4$. This is expected since higher-order correlations in the calculation of the collision frequency have been neglected so far. It should be stressed that a reasonable agreement between analytical and simulated results is achieved only using a complex dynamic collision frequency responsible for the shift and broadening of the plasmon peak.

Special properties of the dynamic structure factor such as sum rules and the high-frequency behavior have been checked. In particular, it is found that a finite value for the third-moment sum rule can be obtained only using a dynamic collision frequency, in contrast to the original Mermin approach based on a frequency-independent relaxation time. The predicted analytical behavior in the high-frequency limit is also seen from the simulation if the numerical accuracy is sufficiently high.

The results presented here are also of importance for the treatment of quantum systems. While an exact treatment of quantum dynamics is out of reach in current numerical simulation techniques, the analytical approach given in this paper allows for a rigorous quantum treatment. On the other hand, the region of applicability of analytical results to strongly coupled plasmas can be found on the basis of comparison with MD simulations as performed in the present work.

ACKNOWLEDGMENT

We would like to thank the DFG for support within the Schwerpunktprogramm SPP1053 ''Wechselwirkung intensiver Laserstrahlung mit Materie'' (Grant No. ZW 57/2-1, Ro 905/15-2).

[1] W. D. Kraeft, D. Kremp, W. Ebeling, and G. Röpke, *Quantum Statistics of Charge Particle Systems* (Plenum, New York, 1986).
[2] H. Reinholz, R. Redmer, G. Röpke, and A. Wierling, Phys. Rev. E **62**, 5648 (2000).
[3] T. Pschiwul and G. Zwicknagel, Contrib. Plasma Phys. **41**, 271 (2001).
[4] T. Pschiwul, Diploma thesis, Erlangen, 2000 (unpublished).
[5] G. Kelbg, Ann. Phys. (Leipzig) **12**, 219 (1963).
[6] C. Deutsch, Phys. Lett. **60A**, 317 (1977); C. Deutsch, M. M. Gombert, and H. Minoo, *ibid.* **66A**, 381 (1978).
[7] J. Lindhard, K. Dan. Vidensk. Selsk. Mat. Fys. Medd. **28**, No. 8 (1954).
[8] N. R. Arista and W. Brandt, Phys. Rev. A **29**, 1471 (1983).
[9] G. D. Mahan, *Many Particle Physics* (Plenum Press, New York, 1990).
[10] R. Redmer, Phys. Rep. **282**, 36 (1997).
[11] H. Reinholz, Ph.D. thesis, Rostock, 1990 (unpublished).
[12] K. Adler, A. Bohr, T. Huus, B. Mottelson, and A. Winther, Rev. Mod. Phys. **28**, 432 (1956).
[13] F. Sigeneger *et al.*, Physica A **152**, 365 (1988).
[14] H. A. Gould and H. E. DeWitt, Phys. Rev. **155**, 68 (1967).
[15] H. Reinholz and G. Röpke, in *Condensed Matter Theories*, edited by A. Anagnostatos and R. F. Bishop (Nova Science, New York, 2000), Vol. 15.
[16] K. L. Kliewer and R. Fuchs, Phys. Rev. **181**, 552 (1969); N. D. Mermin, Phys. Rev. B **1**, 2362 (1970).
[17] D. N. Zubarev, V. Morozov, and G. Röpke, *Statistical Mechanics of Nonequilibrium Processes* (Akademie Verlag, Berlin, 1997).
[18] G. Röpke, A. Selchow, A. Wierling, and H. Reinholz, Phys. Lett. A **260**, 365 (1999).
[19] K. Morawetz and U. Fuhrmann, Phys. Rev. E **61**, 2272 (2000); A. Selchow, G. Röpke, and A. Wierling, Contrib. Plasma Phys. (to be published).
[20] M. P. Allen and D. J. Tildesley, *Computer Simulation of Liquids* (Clarendon Press, Oxford, 1987).
[21] J. P. Hansen, I. R. McDonald, and E. L. Pollock, Phys. Rev. A **11**, 1025 (1975).
[22] J. P. Hansen, I. R. McDonald, and P. Vieillefosse, Phys. Rev. A **20**, 2590 (1979).
[23] P. Schmidt, G. Zwicknagel, P.-G. Reinhard, and C. Toepffer, Phys. Rev. E **56**, 7310 (1997).
[24] B. R. A. Nijboer and F. W. De Wette, Physica (Utrecht) **XXIII**, 309 (1957).
[25] J. P. Hansen, Phys. Rev. A **8**, 3096 (1973).
[26] G. Zwicknagel, Ph.D. thesis, Universität Erlangen, 1994 (unpublished).
[27] G. Zwicknagel, C. Toepffer, and P.-G. Reinhard, Phys. Rep. **309**, 117 (1999).
[28] W. H. Press, B. P. Flannery, S. A. Teukolsky, and W. T. Vetterling, *Numerical Recipes* (Cambridge University Press, Cambridge, 1989).